

Mathematical Modeling of Plasma Transport in a Helical Magnetic Field

Corresponding Member of the RAS G. G. Lazareva^{a,*}, I. P. Oksogoeva^{a,**}, and A. V. Sudnikov^{b,***}

Received August 3, 2023; revised September 1, 2023; accepted November 3, 2023

Abstract—The paper presents the results of mathematical modeling of plasma transport in a spiral magnetic field using new experimental data obtained at the SMOLA trap created at the Budker Institute of Nuclear Physics of the Siberian Branch of the Russian Academy of Sciences. Plasma confinement in the trap is carried out by transmitting a pulse from a magnetic field with helical symmetry to a rotating plasma. A new mathematical model is based on a stationary plasma transport equation in an axially symmetric formulation. The distribution of the plasma concentration obtained by numerical simulation confirmed the confinement effect obtained in the experiment. The dependences of the integral characteristics of the plasma on the depth of corrugation of the magnetic field, diffusion, and plasma potential are obtained. The mathematical model is intended to predict plasma confinement parameters in designing traps with a spiral magnetic field.

Keywords: mathematical modeling, transport equation, helical magnetic field

DOI: 10.1134/S1064562423701508

1. INTRODUCTION

Numerical simulation of plasma flow in a magnetic field based on complicated mathematical models involving the description of numerous subtle effects has a long history [1–6] and significant achievements. These studies are of great interest for controlled thermonuclear fusion, the study of resistance of materials to the influence of high thermal loads, laboratory modeling of astrophysical processes, and a number of other fundamental and real-world scientific problems.

The main method for plasma thermal insulation is its confinement in a magnetic field of various configurations. The greatest progress has been made in field and numerical experiments [7–9] for systems with a toroidal magnetic field. Modern advances in mathematics in this field have reached a very high level, and open-source packages for mathematical modeling of such systems have been created.

An alternative approach is plasma confinement in open magnetic systems, where the field is close to axisymmetric and its field lines cross the boundary of the confinement region at two points [10]. The advantages of this approach include more effective use of

magnetic field energy, scalability, and the engineering simplicity of the system. The main scientific goal of the physics of open traps is to reduce the loss of particles and energy along magnetic field lines in area where they leave the confinement region. Great progress has been made in understanding the physics of open magnetic configurations and achieved plasma parameters [11]. Contributions to these achievements were made by mathematical modeling of plasma confinement based on multiple-mirror traps [12–14].

The diversity and complexity of plasma flow parameters dictate the need for specialized models of different processes. There is no universal model. Mathematical models of plasma physics are characterized by different spatial and temporal scales and process characteristics. These models typically combine continuum mechanics equations with allowance for electromagnetic forces and Maxwell's equations. Depending on the choice of approximation, it is possible to distinguish kinetic, magnetohydrodynamic, and transport plasma models [15].

Plasma confinement by a helically symmetric magnetic field was proposed as a development of multiple-mirror trap confinement [16]. In a frame of reference attached to the rotating plasma, the motion of magnetic perturbations has a velocity component codirectional with the magnetic field, so momentum can be transferred to trapped particles. Collisions between passing and trapped particles produce an effective force that acts on the plasma as a whole and facilitates returning the ions to the confinement region.

^a Peoples' Friendship University of Russia, Moscow, Russia

^b Budker Institute of Nuclear Physics, Siberian Branch, Russian Academy of Sciences, Novosibirsk, Russia

*e-mail: lazareva-gg@rudn.ru

**e-mail: oksogi@mail.ru

***e-mail: a.v.sudnikov@inp.nsk.su

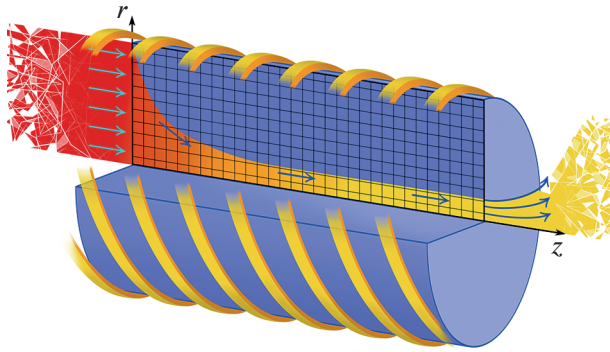


Fig. 1. Schematic of the central part of the trap. The computational domain in a cross section of the trap, spiral magnets (yellow), and plasma flow (red-yellow).

The SMOLA spiral magnetic open trap was designed and constructed in 2017 at the Budker Institute of Nuclear Physics of the Siberian Branch of the Russian Academy of Sciences for experimental verification of this idea [17, 18]. Plasma in the SMOLA trap is confined by a classical mirror, as well as by a multiple-mirror section with a helical magnetic field. The experiment involves variations in parameters, such as the axial magnetic field, the ratio of the axial to helical magnetic fields, and the density and angular velocity of the plasma. The SMOLA trap is designed to simulate effects of helical plasma confinement at low (and, hence, easily achievable) plasma temperatures. To scale helical mirror confinement to thermonuclear systems, is necessary to perform a detailed comparison of experimentally observed plasma flows with simulated ones and further computations of the effectiveness of a larger-scale system based on a mathematical model. Currently, agreement between observed results and approximate theoretical estimates has been shown. However, there is no exact analytical solution for the theory of helical plasma confinement, so comparisons can rely on results of the numerical solution of the equations of plasma motion.

A mathematical model of plasma transport in a helical magnetic field was constructed using the equations from [17–19] and the parameters of the SMOLA trap. The mathematical modeling of the process was first carried out in [20]. A development of this new research direction is the determination of parameters of the process that cannot be measured experimentally and the use of magnetic fields of complex geometry in the computations. The goal of this study is to predict the confinement parameters at the stage of trap design.

2. FORMULATION OF THE PROBLEM

In the modeled experiment, the parameters of the plasma and the electromagnetic field reach a steady state over 40 ms, this state persists for 120 ms, after

which the discharge is switched off. The main goal of the experiments and mathematical modeling was to examine plasma confinement modes in which all parameters are constant. Consider the motion of the plasma in the central part of the trap, which has the shape of a cylinder (see Fig. 1). The substance injected by the plasma source enters the confinement region through the left cylinder base and goes out into the expanding section through its right base. The plasma flow is axisymmetric, so our consideration can be restricted to a two-dimensional problem formulation [21]. Thus, plasma confinement in a spiral magnetic field is described by stationary equations in a cross section of the central part of the trap in the (r, z) plane.

Expressions for radial and axial transport of particles in a helical magnetic field are obtained in [19]. The system of equations describes the dynamics of the plasma in the MHD approximation in an axially symmetric formulation. The differences in the motion of trapped and passing ions are taken into account in the form of an effective friction force depending on the relative velocity of the components and the fraction of trapped particles. The axial force acting on the plasma results from the interaction of the radial electric current of trapped ions with the azimuthal component of the helical magnetic field. The diffusion of the plasma across the magnetic field is taken into account. By eliminating dependent variables, the system of equations is reduced to the continuity equation of the flow.

Consider the domain $[0, r_{\max}] \times [0, z_{\max}]$ in a cross section of the central part of the trap (Fig. 1). In dimensionless variables, the domain is a unit square. Assume that the plasma does not reach the trap walls. A symmetry condition is set on the z axis, and boundary plasma concentration distributions $u(r, 0) = u_L(r)$ and $u(r, z_{\max}) = u_R(r)$ are specified at the inlet and outlet of the plasma flow. In the computations, we used experimental data on boundary concentration distributions [11] (Fig. 2a). Thus, the stationary problem has the form

$$\left\{ \begin{aligned} & \frac{l}{x(r)\partial z \Lambda} \frac{\partial(T(r)u(r, z))}{\partial z} + l(1+x(r)) \frac{\partial(\Phi(r, z)\zeta(r)u(r, z))}{\partial z} \\ & + \frac{\partial}{\partial r} lZ^{-1}\zeta(r) \frac{\partial(T(r)u(r, z))}{\partial z} + \frac{\partial}{\partial r} lD \frac{\partial u}{\partial r} = 0 \\ & \frac{\partial u}{\partial r}(0, z) = 0, \quad u(r, 0) = u_L(r) \\ & \frac{\partial u}{\partial r}(1, z) = 0, \quad u(r, 1) = u_R(r). \end{aligned} \right. \quad (1)$$

Here, u is the plasma concentration; $T = T_i + T_e$, where $T_i = 4$ eV and $T_e = 30(1 - (r/r_0)^2)$ are the ion and electron temperatures, respectively; Λ is the ratio of the length of the system to the ion free path Λ ; $\kappa(r, R_m)$ is the fraction of trapped particles; $l = 216$ cm is the length of the system along the field lines; Z is the average charge number of an ion; and D is the diffu-

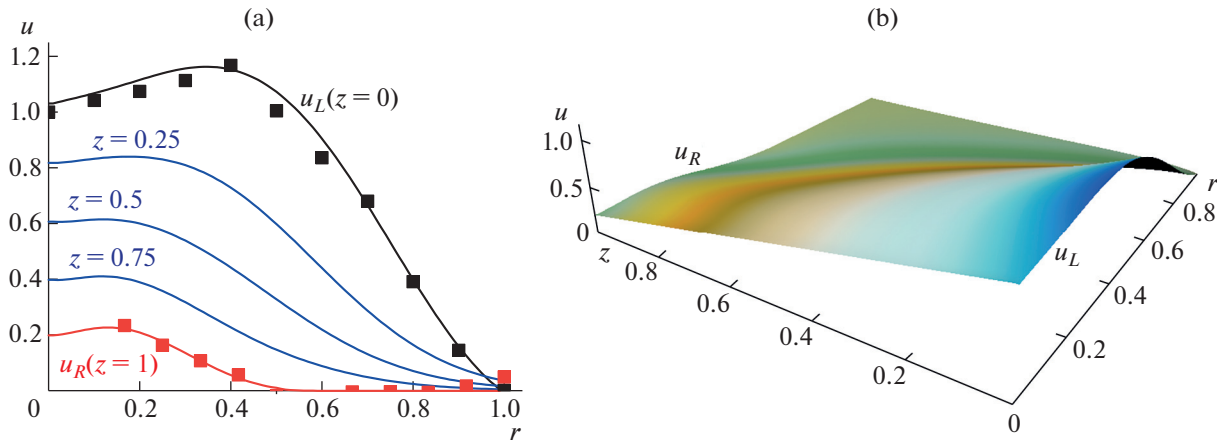


Fig. 2. (a) Plasma concentration in cross sections of the z axis: computed (curve) and experimental (squares) boundary plasma distributions at the inlet (black) and the outlet (red) and the computed plasma distribution inside the domain (blue curves). (b) Plasma concentration distribution over the computational domain.

sion coefficient in the transverse field. The fraction of trapped particles is given by $\kappa(r, R_m) = 1 - 1/R(r, R_m)$, where $R(r, R_m) = 2(R_m - 1)(r/a)^2 + 1$ and $R_m = 1.52$ is the corrugation depth. The parameter $\zeta = c/V_z$ is the ratio of the speed of sound $c_s = (T_e/M)^{1/2}$ and the axial velocity V_z of magnetic perturbations in the plasma rotating in its own ambipolar electric field. In Eq. (1), the physical quantities are nondimensionalized using $r_0 = a$, $z_0 = l$, $\phi_0 = T_e/e$, $u_0 = u_{\max}$, and $T_0 = T_e$, where $a = 8$ cm is the boundary of the chamber where a plasma can exist.

It is well known that the plasma potential reduces with increasing z due to the transverse conductivity of the plasma. Its spatial distribution is specified as the derivative of the electric field magnitude decreasing along the axis (Fig. 3a): $\Phi(r, z) = \left(1 - \frac{0.002z}{h}\right) \frac{\partial |\phi(r)|}{\partial r}$. In experiments with the SMOLA trap, the plasma potential measured with probes depends on experimental parameters. The maximum of ϕ varies from $2T_e/e$ to $3T_e/e$. The maximum value of the dimensionless potential ϕ for next generation devices in which helical confinement is possible also lies within this range [22, 23]. The experimentally observed potential distribution in the central plasma region (for dimensionless radius values smaller than 0.6) is close to quadratic distribution. In the peripheral region of the plasma, the derivative of the potential with respect to radius decreases. The measurement error of the potential in the experiment is about 5%. The degree and coefficients of the approximating polynomial are chosen so that the deviation from its values measured in a reference experiment is comparable to the experimental error.

3. SOLUTION METHOD

Problem (1) was solved using time marching to a steady state [20] and a lower cost overrelaxation method [24] with the relaxation parameter $\omega = 2 - O(h)$ and the mixed derivative approximated on a stencil [25]. Note that problem (1) involves the parameter $\zeta(r) = 1/Ar$ obtained by approximation of experimental data; here, $A = 20$. On the axis at $r = 0$, the parameter ζ is bounded by the value at $r = \rho_B$, where $\rho_B = V_T mc/eB$ is the Larmor radius. For the parameters of the SMOLA trap, we have $\rho_B \approx 0.3-0.4$ cm. This is explained by the fact that an ion moves on a Larmor orbit (rotates in the magnetic field), so its radial coordinate oscillates. In the considered model, all influences are averaged, and an ion is assigned the coordinate of the center of the circle on which it moves in the magnetic field. In other words, the coordinate vanishes for ions that move in a circle at a distance of the Larmor radius from its center. Accordingly, to avoid singularities of the solution in the computations near the axis of symmetry, the dimensionless parameter ζ is specified as

$$\zeta(r) = \begin{cases} 1/Ar, & r > \rho_B \\ 1/A\rho_B, & \rho_B \geq r \geq 0. \end{cases}$$

Along with other advantages, the relaxation method is convenient for use in cylindrical coordinates. The sought element is expressed in terms of neighboring ones according to a five-point stencil, which is a universal approach independent of the choice of a coordinate system.

Figure 2a shows experimental values of the plasma concentration at the inlet (squares) and the outlet (circles) and their interpolations of the form

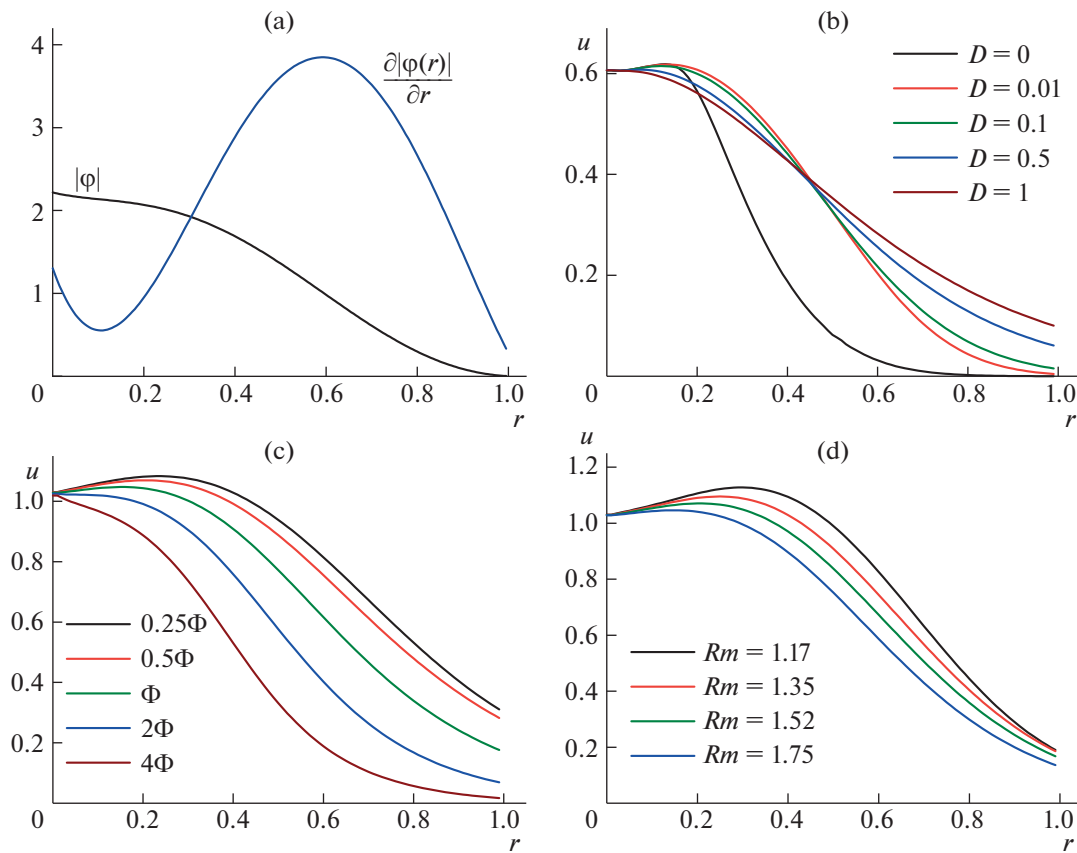


Fig. 3. (a) Magnitude of the electric field potential (black) and its derivative (blue) as functions of the trap radius. Plasma concentration distribution at $z = 0.4$ for various values of (b) diffusion coefficient, (c) derivative of the electric field magnitude, and (d) corrugation depth.

$$u_L(r) = 1.03 + 0.46r - 1.52r^2 + 14.48r^3 - 44.17r^4 + 43.77r^5 - 14.05r^6,$$

$$u_R(r) = 0.2 - 0.12r + 9.11r^2 - 73.43r^3 + 210.13r^4 - 285.64r^5 + 188.54r^6 - 48.78r^7.$$

The electric field potential $\varphi(r)$ was specified as a polynomial (Fig. 3a) interpolating the experimental data:

$$\varphi(r) = -2.21776 + 1.31r - 7.79r^2 + 31.18r^3 - 33.43r^4 + 10.94r^5.$$

4. SIMULATION RESULTS

Plasma concentration distributions for various values of the corrugation depth, diffusion, and plasma transport in a helical magnetic field. For a further analysis of the numerical results and for comparison of them with experimental data, we present distributions at cross sections along the z axis (Fig. 2a). The plasma concentration distribution over the computational

domain, which is a unit square in dimensionless form, is displayed in Fig. 2b. The numerical results show a decrease in the plasma density, which confirms the confinement effect observed in the experiments.

In the experiment, the sensor measuring the plasma concentration is placed at $z = 0.4$. Accordingly, Fig. 3 presents the numerical results only in this cross section. Numerical experiments were carried out for various admissible values of the diffusion coefficient, the derivative of the electric field magnitude, and corrugation depth. The results show that the plasma is compressed toward the axis as the diffusion coefficient decreases in the transverse field. Taking into account the finite experimental error, the computed distributions were found to agree with the experimental ones for diffusion coefficient values in the range $D = 0.01 - 0.1$. The subsequent computations were carried out with $D = 0.1$. As the derivative of the electric field magnitude and the corrugation depth increase, the plasma column is compressed toward the axis. These results agree with the experimental data. In the future, the described method can be used to predict the performance of available and potential devices for plasma confinement in a helical magnetic field. A major task

for this prediction would be the correct specification of boundary conditions and numerical coefficients in the transport equation without using a priori known experimental distributions of plasma characteristics. For this purpose, we intend to perform computations with a known exact boundary condition at infinity. The solution value at $z = 1$ would be used as the plasma density distribution at the outlet of the improved confinement section.

5. CONCLUSIONS

A mathematical model of plasma transport in the SMOLA spiral magnetic open trap has been presented. The integral plasma density was obtained as a function of the magnetic field corrugation depth, diffusion, and the plasma potential. The simulated dependences were found to agree with experimental data for the dimensionless diffusion coefficient $D = 0.01\text{--}0.1$ and the cross-section-averaged corrugation depth $R_m = 1.52$. The computations revealed a pinch effect (a decrease in the mean radius of the plasma column), which was also observed in the experiment. Further research will aim at expanding the range of parameters in which the model has a sufficient predictive power.

FUNDING

This work was supported by the Ministry of Science and Higher Education of the Russian Federation, megagrant agreement no. 075-15-2022-1115.

CONFLICT OF INTEREST

The authors of this work declare that they have no conflicts of interest.

REFERENCES

1. A. A. Samarskii, "Numerical methods for solving multi-dimensional problems of mechanics and physics," *USSR Comput. Math. Math. Phys.* **20** (6), 52–99 (1980).
2. K. V. Brushlinskii and V. V. Savelyev, "Magnetic traps for plasma confinement," *Mat. Model.* **11** (5), 3–36 (1999).
3. Yu. N. Dnestrovskii and D. P. Kostomarov, *Numerical Simulation of Plasmas* (Springer-Verlag, New York, 1986).
4. C. K. Birdsall and A. B. Langdon, *Plasma Physics via Computer Simulations* (McGraw-Hill, New York, 1985).
5. Yu. S. Sigov, *Numerical Experiment: A Bridge between the Past and Future of Plasma Physics* (Fizmatlit, Moscow, 2001) [in Russian]. (Fizmatlit, Moscow, 2001) [in Russian].
6. Yu. A. Berezin and G. I. Dudnikova, *Numerical Plasma Models and Reconnection Processes* (Nauka, Moscow, 1985) [in Russian].
7. K. V. Brushlinskii and I. A. Kondrat'ev, Preprint No. 20, IPM RAN (Keldysh Inst. of Applied Mathematics, Russian Academy of Sciences, Moscow, 2018).
8. B. Cohen, D. Barnes, J. Dawson, G. Hammett, W. Lee, G. Kerbel, J. Leboeuf, P. Liewer, T. Tajima, and R. Waltz, "The numerical tokamak project: Simulation of turbulent transport," *Comput. Phys. Commun.* **87** (1–2), 1–15 (1995).
9. R. Gruber, L. M. Degtyarev, A. Kuper, A. A. Martynov, S. Yu. Medvedev, and V. D. Shafranov, "Three-dimensional plasma equilibrium model based on the poloidal representation of the magnetic field," *Plasma Phys. Rep.* **22** (3), 186–194 (1996).
10. A. V. Burdakov and V. V. Postupaev, "Multiple-mirror trap: A path from Budker magnetic mirrors to linear fusion reactor," *Phys.-Usp.* **61** (6), 582–600 (2018).
11. P. A. Bagryansky, A. D. Beklemishev, and V. V. Postupaev, "Encouraging results and new ideas for fusion in linear traps," *J. Fusion Energy* **38**, 162–181 (2019).
12. E. A. Berendeev, G. I. Dimov, G. I. Dudnikova, A. V. Ivanov, G. G. Lazareva, and V. A. Vshivkov, "Mathematical and experimental simulation of a cylindrical plasma target trap with inverse magnetic mirrors," *J. Plasma Phys.* **81** (5), 495810512 (2015).
13. A. Yu. Perepelkina, V. D. Levchenko, and I. A. Goryachev, "Three-dimensional kinetic code CFHall for modeling a magnetized plasma," *Mat. Model.* **25** (11), 98–110 (2013).
14. V. T. Asterlin, A. V. Burdakov, and V. V. Postupaev, "Modeling the dynamics of a dense emitting plasma cluster in the GOL-3-II device," *Sib. Zh. Ind. Mat.* **1** (2), 45–50 (1998).
15. N. N. Kalitkin and D. P. Kostomarov, "Mathematical models of plasma physics (survey)," *Mat. Model.* **18** (11), 67–94 (2006).
16. A. D. Beklemishev, "Helicoidal system for axial plasma pumping in linear traps," *Fusion Sci. Technol.* **63** (1), 355–357 (2013).
17. V. V. Postupaev, A. V. Sudnikov, A. D. Beklemishev, and I. A. Ivanov, "Helical mirrors for active plasma flow suppression in linear magnetic traps," *Fusion Eng. Des.* **106**, 29–31 (2016).
18. A. V. Sudnikov, I. A. Ivanov, A. A. Inzhevatkina, M. V. Larichkin, K. A. Lomov, V. V. Postupaev, M. S. Tolkachev, and V. O. Ustyuzhanin, "Plasma flow suppression by the linear helical mirror system," *J. Plasma Phys.* **88** (1) (2022).
19. A. D. Beklemishev, "Radial and axial transport in trap sections with helical corrugation," *AIP Conf. Proc.* **1771**, 040006 (2016).
20. G. G. Lazareva, I. P. Oksogoeva, and A. V. Sudnikov, "Mathematical modeling of plasma transport in a helical magnetic field," *Lobachevskii J. Math.* **43** (10), 2685–2691 (2022).
21. K. V. Brushlinskii and N. S. Zhdanova, "Computation of axisymmetric MHD flows in a channel with an external longitudinal magnetic field," *Comput. Math. Math. Phys.* **46** (3), 527–536 (2006).

22. A. V. Sudnikov, A. D. Beklemishev, V. V. Postupaev, A. V. Burdakov, I. A. Ivanov, N. G. Vasilyeva, K. N. Kuklin, and E. N. Sidorov, “SMOLA device for helical mirror concept exploration,” *Fusion Eng. Des.* **122**, 86–93 (2017).
23. D. I. Skovorodin, I. S. Chernoshtanov, V. Kh. Amirov, et al., Preprint of IYaF (Budker Institute of Nuclear Physics, Sib. Branch, Russ. Acad. Sci., Novosibirsk, 2023).
24. A. A. Samarskii and E. S. Nikolaev, *Numerical Methods for Grid Equations* (Nauka, Moscow, 1978; Birkhäuser, Basel, 1989).
25. A. A. Samarskii, V. I. Mazhukin, P. P. Matus, and G. I. Shishkin, “Monotone difference schemes for equations with mixed derivatives,” *Mat. Model.* **13** (2), 17–26 (2001).

Translated by I. Ruzanova

Publisher’s Note. Pleiades Publishing remains neutral with regard to jurisdictional claims in published maps and institutional affiliations.